Pre-eruptive migration of earthquakes at the Piton de la Fournaise volcano (Réunion Island)

Jean Battaglia, Valérie Ferrazzini, Thomas Staudacher, Keiiti Aki, Jean-Louis Cheminée

▶ **To cite this version:**

Jean Battaglia, Valérie Ferrazzini, Thomas Staudacher, Keiiti Aki, Jean-Louis Cheminée. Pre-eruptive migration of earthquakes at the Piton de la Fournaise volcano (Réunion Island). Geophysical Journal International, 2005, 161, pp.549-558. 10.1111/j.1365-246X.2005.02606.x . insu-03601118

HAL Id: insu-03601118
https://insu.hal.science/insu-03601118

Submitted on 8 Mar 2022

HAL is a multi-disciplinary open access archive for the deposit and dissemination of scientific research documents, whether they are published or not. The documents may come from teaching and research institutions in France or abroad, or from public or private research centers.

L'archive ouverte pluridisciplinaire **HAL**, est destinée au dépôt et à la diffusion de documents scientifiques de niveau recherche, publiés ou non, émanant des établissements d'enseignement et de recherche français ou étrangers, des laboratoires publics ou privés.

Distributed under a Creative Commons Attribution 4.0 International License

Geophys. J. Int. (2005) **161,** 549–558 doi: 10.1111/j.1365-246X.2005.02606.x

Pre-eruptive migration of earthquakes at the Piton de la Fournaise volcano (Réunion Island)

Jean Battaglia,[1,*] Valérie Ferrazzini,[1] Thomas Staudacher,[1] Keiiti Aki[1] and Jean-Louis Cheminée[2]

[1]*Observatoire Volcanologique du Piton de la Fournaise, Institut de Physique du Globe de Paris,* 14 RN3, 97418 *La Plaine des Cafres, La Réunion, France E-mail: battag@na.infn.it*

[2]*Observatoires Volcanologiques, Institut de Physique du Globe de Paris* - B89, 4 *Place Jussieu,* 75252 *Paris cedex* 05, *France*

Accepted 2005 February 8. Received 2005 January 20; in original form 2004 August 31

SUMMARY

We present a study of the seismicity which preceded the 1998 March 9 eruption of the Piton de la Fournaise volcano. The eruption was preceded by a seismic crisis unusually long for this volcano which lasted for more than 35 hr and included about 3100 events with a maximum magnitude of 2.2. We located 583 volcano-tectonic (VT) events by manually picking their arrival times. The locations outline a monotonic upward migration of the hypocentres from about 5 km below sea level to the surface, leading to the onset of the eruption. This good correlation of the seismicity with eruptive activity suggests that the seismic migration was triggered by the ascent of magma toward the eruption site. The location of the earthquakes outlines an almost vertical conduit below the volcano providing new insights into the volcanic plumbing system.

Key words: volcano seismicity, eruption, earthquake migration, Piton de la Fournaise.

1 INTRODUCTION

Volcanic eruptions are nearly always preceded by an increase in seismic activity (Benoit & McNutt 1996). For this reason, seismology has become a major tool for monitoring and forecasting the activity of volcanoes. The activity almost always includes high-frequency tectonic events related to rock fracture induced by magma migrating inside the volcanic edifice. Such events can be located by picking their arrival times and using standard location techniques. The activity also often includes signals typical of active volcanoes such as long-period events or tremors which are directly related to fluid transport (Chouet 1996) but whose sources are usually difficult to locate precisely using standard location techniques due to their emergent onsets.

Since eruptions are caused by the migration of magma towards the surface, we may expect such a process to be accompanied by simultaneously migrating earthquakes. Well-documented cases of such phenomena are, however, rare and are mostly limited to basaltic volcanoes. Horizontal pre-eruptive migrations of earthquakes have been observed in rift zones at Krafla volcano, Iceland (Brandsdóttir & Einarsson 1979) and Kilauea, Hawaii (Koyanagi *et al.* 1988; Rubin *et al.* 1998). Vertical migrations have been reported preceding the 1989 submarine Ito Oki eruption (Ukawa & Tsukahara 1996) and prior to the 1989 Unzen volcanic eruption (Umakoshi *et al.* 2001). A spectacular case of earthquake migration attributed to magma propagating away and downwards from the volcanic centre was observed at the beginning of the 2000 June–July eruption of Miyake-Jima (Toda *et al.* 2002).

More commonly, especially in silicic volcanoes, the seismicity does not outline the path of magma propagating towards the eruption site. Discontinuously shallowing seismicity has been observed prior to the onset of several eruptions. At Mount Pinatubo, VT seismicity preceding the 1991 June 15 eruption was first focused in a single cluster located about 5 km from the summit and shifted to a second shallower cluster below the summit 2 weeks before the beginning of the eruption (Harlow *et al.* 1996). Similarly, shallowing of the VT seismicity has been observed preceding the 1998 November eruption of Colima volcano (Zobin *et al.* 2002). Frequently, the presence of several distinct clusters of earthquakes has been observed, but their direct relation with volcanic activity is difficult to establish. At Guagua Pichincha, the 1998–1999 eruptive activity was preceded and accompanied by two swarms of activity, one situated below the volcano and a second, deeper, about 15–20 km from the first one (Legrand *et al.* 2002). Distinct clusters were observed prior to the 1984 and 1992 eruptions of Merapi volcano (Ratdomopurbo & Poupinet 2000) and in Montserrat (Aspinall *et al.* 1998; Gardner & White 2002). They may occur in places of stress concentration, but not necessarily where magma moves inside the volcanic edifice. In many cases the pre-eruptive seismicity is mostly focused below the eruptive vent or volcano summit as for Mount St Helens (Endo *et al.* 1981) or Popocatepetl (Arciniega-Ceballos *et al.* 2000). The 1989 eruption of Redoubt (Power *et al.* 1994) was

*Now at: Dipartimento di Scienze Fisiche, Università degli Studi di Napoli Federico II, Via Coroglio 156, 80124 Napoli, Italy. E-mail: battag@na.infn.it.

© 2005 RAS

Downloaded from https://academic.oup.com/gji/article/161/2/549/1958870 by CNRS - ISTO user on 08 March 2022

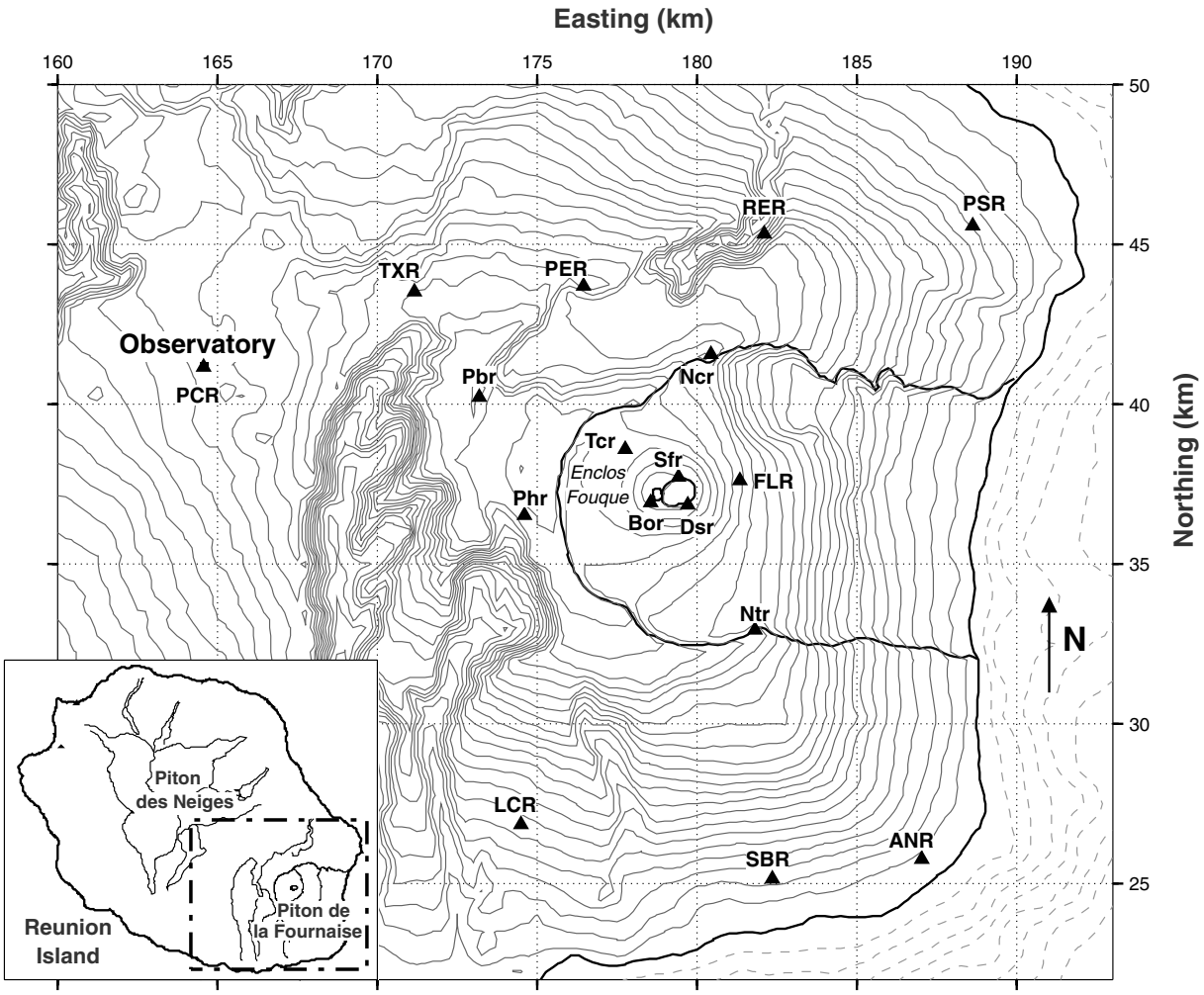

Figure 1. Map of the eastern part of Réunion Island with the seismic stations of the monitoring network represented as triangles. Geographical coordinates are Gauss–Laborde kilometric coordinates (transverse Mercator) and isolines are spaced every 200 m.

preceded by a swarm which included thousands of shallow long-period (non-tectonic) events but no detected VT events.

No case of well-documented upward and monotonic migration clearly illustrating the ascent of magma from depth prior to an eruption could be found. A possible reason for the lack of such observations is found in the poor station coverage on many of the world's active volcanoes and relatively small numbers of published cases. Available observations suggest, however, that vertical migrations are very uncommon while horizontal migrations appear to be more frequent.

2 BACKGROUND

Piton de la Fournaise is a basaltic volcano which occupies the eastern part of Réunion Island, in the western Indian Ocean (21°07′S – 55°32′E). The central cone (2631 m) of the volcano (Fig. 1) lies in a caldera-like depression called the Enclos Fouqué which is open to the east towards the ocean. Piton de la Fournaise is highly active with a mean time between eruptions of about 10 months during the last two centuries (Stieltjes & Moutou 1989) and at least 125 recorded eruptions during the last century. Most of the eruptions occur along fissures inside the Enclos Fouqué.

Since 1980 the Piton de la Fournaise has been monitored by an observatory installed about 15 km from the summit of the volcano. In 1998 the permanent network included seismic, deformation, magnetic and radon measurements. Between 1980 and 1992, 28 eruptions occurred and most of them were only preceded by short-duration seismic crises including only several tens of VT events situated below the central cone, above sea level (Lénat *et al.* 1989a,b; Hirn *et al.* 1991). More generally, most of the recorded seismicity during that period had a low magnitude (below 2.5), was shallow and was located below the summit. Fig. 2 presents an example of the seismicity recorded during the entire period from 1996 January to the onset of the 1998 March 9 pre-eruptive crisis: except for two small clusters below sea level all the seismicity is found above sea level.

This absence of deeper seismicity has been interpreted by Lénat & Bachèlery (1990) as due to the absence of continuous deep magma transfers. They proposed the model of a summit reservoir composed of a large number of relatively small independent magma pockets extending from several hundred metres below the surface to sea level. In this model, the frequent small eruptions are caused by the emptying of those magma pockets which are only periodically refilled by deeper magma transfers. The 1977 eruption is unique with

Downloaded from https://academic.oup.com/gji/article/161/2/549/1995870 by CNRS - ISTO user on 08 March 2022

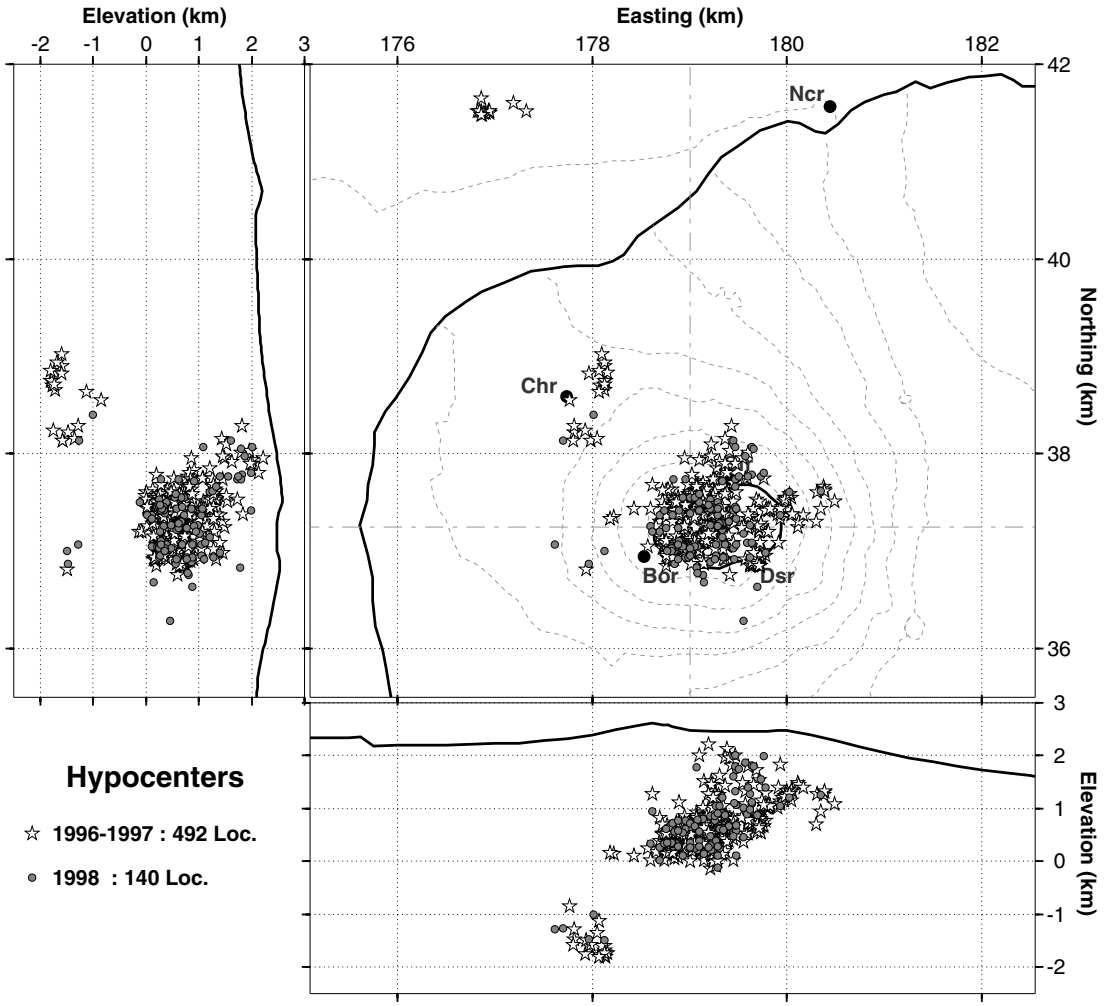

Figure 2. Location of volcano tectonic events which occurred between 1996 and the 1998 March 9 eruption. Map view and north–south and east–west cross-sections are presented. The events located in the upper left part of the figure are found about 16 km below sea level and do not appear on the vertical cross-sections.

regard to those which occurred until 1998 as it was a major oceanite (basalt with high percentage of olivine) eruption like those which occurred in 1931 and 1961. It is interpreted as corresponding to a refilling of the summit system. This hypothesis is also suggested by the petrological and chemical similarity of the lava emitted since 1977. Unfortunately, as the observatory was not yet installed, no information is available concerning the evolution of the seismicity or deformation prior to the beginning of the 1977 eruption. The presence of a magma chamber just below sea level is suggested by the presence of a low-velocity zone (Sapin *et al.* 1996; Nercessian *et al.* 1996). Eruptions may be caused by crystallization (Tait *et al.* 1989) in that chamber which may expel small magma pockets situated above.

The period of high eruptive activity until 1992 was followed by an unusually long period without eruption which lasted from September 1992 until March 1998. The seismicity of VT events declined between 1992 and 1996. The summit activity started increasing in 1996 and several earthquakes were observed at a depth about 16 km below sea level, about 10 km north-northwest of the summit (Fig. 2). In particular, a cluster of such deep events, with similar waveforms, occurred in 1996 September. In 1996 November a first swarm of shallow events occurred below the summit followed by a general increase of the background seismicity below the summit during 1997 and by a second small swarm of shallow events in 1997 August.

After five and half years of dormancy, the Piton de la Fournaise volcano started erupting on 1998 March 9 at 11:05 UT (Staudacher *et al.* 1998). The eruption, which occurred along *en echelon* fissures on the northern flank of the summit cone (Fig. 3), was preceded by a pre-eruptive crisis which included more than 3100 VT events and lasted for about 35 hr, which is unusually long for this volcano (Aki & Ferrazzini 2000). The onset of this eruption was followed at the end of March 11 by a second eruption which occurred southwest of the summit at crater Hudson.

3 DATA

We use data from the local monitoring network of the Observatoire Volcanologique du Piton de la Fournaise. At the time of our study, the seismic network was composed of 19 stations, the locations of which are shown in Fig. 1. Except for stations PCR and RER, which

Downloaded from https://academic.oup.com/gji/article/161/2/549/1995870 by CNRS - ISTO user on 08 March 2022

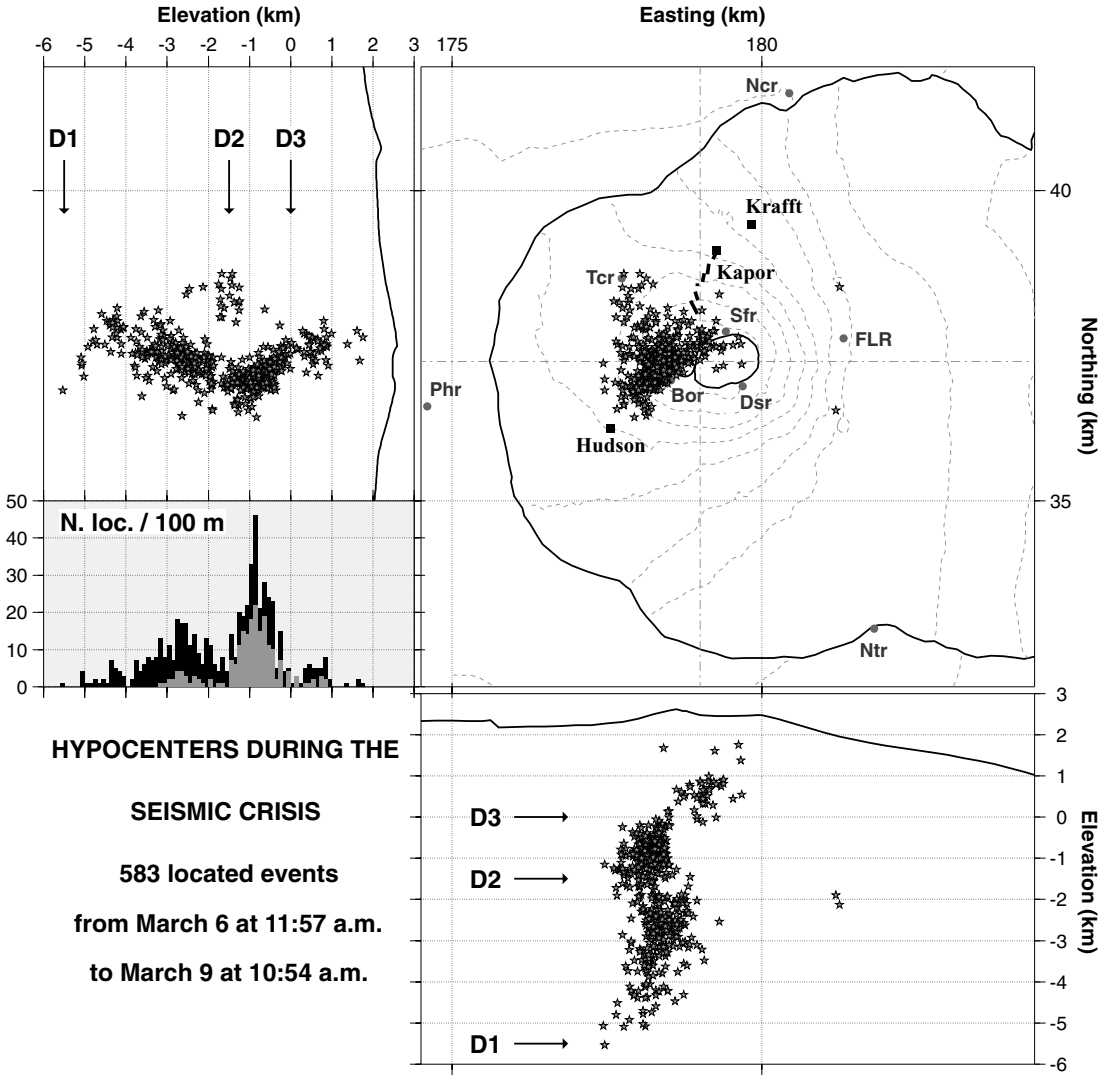

Figure 3. Geographical location of the hypocentres during the pre-eruptive seismic crisis. The earthquakes have been located using HYPO71 software with an eight-layer velocity model. The histogram inserted on the north–south cross-section shows in black the number of locations as a function of the depth considering intervals of 100 m; superposed in grey is the same but only considering events with a magnitude greater that 1.5. Eruption fissures and craters are indicated.

are Geotech SL210, all stations are equipped with Mark Products L4 short-period seismometers with a corner frequency at 1 Hz. The Geotech SL210 are larger-band seismometers. All stations measure the vertical ground velocity and only three stations have horizontal components (Pbr, TCR and Bor). Stations are telemetered in real time to the observatory and recorded digitally with a 100 Hz sampling frequency. Only triggered data are available.

To locate the earthquakes during the pre-eruptive crisis, we manually picked their arrival times at the different stations of the network. *P* waves were only picked on vertical components and *S* waves on the horizontal ones. The software HYPO71 (Lee & Lahr 1975), modified to take into account the station elevation, has been used to determine the hypocentres for 583 sufficiently large events using a 1-D velocity model composed of eight horizontal layers which has been developed for routine hypocentre determination at the observatory (Table 1). To test the influence of the velocity model on the locations, including possible clustering at the boundaries of the velocity layers, we compared our results with locations obtain after changing the velocity model.

Table 1. Velocity model used for the location of hypocentres; depths of the layers boundaries are given in kilometres with negative values for layers above sea level.

V_p	Depth (km)
3.50	−2.70
3.70	−0.79
4.20	0.2
4.50	2.2
5.00	4.2
6.50	17.0
6.80	20.0
8.00	30.0

4 PRE-ERUPTIVE SEISMICITY

The spatial distribution of the locations is presented in Fig. 3 and the time evolution of the focal depth in Figs 4 and 5. The spatial

Downloaded from https://academic.oup.com/gji/article/161/2/549/1995870 by CNRS - ISTO user on 08 March 2022

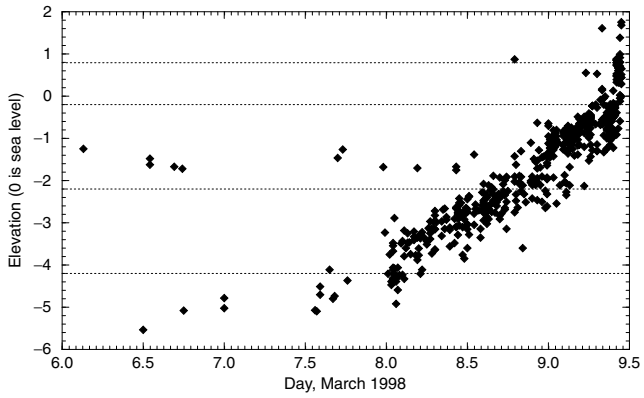

Figure 4. Evolution of the focal depth for earthquakes located between the beginning of March 7 and the onset of the eruption at 11:00 on 1998 March 9. The boundaries of the layers of the velocity model used for location are indicated by light horizontal lines.

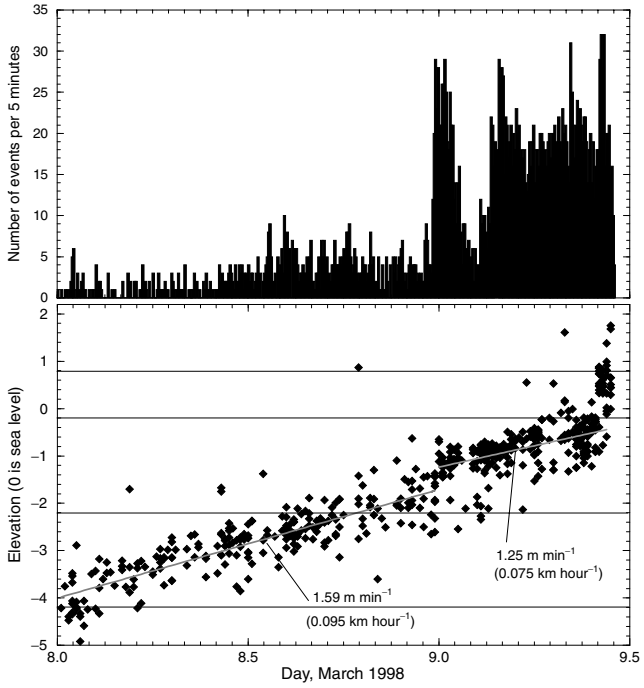

Figure 5. Number of volcano-tectonic events per 5 min (upper plot) and evolution of the focal depth of the 583 located hypocentres (lower plot). Continuous lines on the lower plot are linear regressions corresponding to the mean migration rates.

and temporal evolution of the hypocentres is described in Figs 6 and 7.

The first group of events directly related to the precursory seismic crisis started on March 6 and 7. About 20 earthquakes occurred during those two days and were mainly clustered around two levels (Fig. 4). The first one was situated under station Tcr between 1 and 2 km below sea level (bsl), at the place where an isolated cluster of seismicity was observed during the 2 yr preceding the eruption (Fig. 2). The second group was located around 5 km bsl (the deepest event being around 5.5 km bsl) and appears as the lower extension of the nearly vertical path described by most of the pre-eruptive seismicity (Fig. 3). The approximate starting depth of 5–6 km has been recognized as a major geological discontinuity (noted D1 hereafter) as it corresponds to the top of the pre-existing oceanic crust upon which the volcanic edifice is built according to results of the reflection–refraction seismic survey FOURNASEIS (Gallart *et al.* 1999). This depth is shallower than expected from the flexure model and implies the absence of significant downward flexure beneath the island.

Beginning around 00:00 on March 8, the activity started to increase leading to the eruption 35 hr later. During March 8, the seismicity remained relatively steady and the depth of the hypocentres slowly moved towards the surface with a steady migration velocity of about 1.59 ± 0.06 m min^{-1} (0.095 km hr^{-1}) (Fig. 5). Around 1.5 km depth a discontinuity (D2) is observed in the migration with the presence of a low-seismicity zone which is not apparently an artefact of the velocity model used for the location of the earthquakes. In space, discontinuity D2 also corresponds to the depth at which persistent seismicity is observed during March 6, 7 and 8, as well as during the years 1996 and 1997, mainly clustered below station Tcr, separate from the main path of migration (Fig. 2). Also, a major change is observed in the orientation of the migration at the depth of D2 (particularly clear on the north–south cross-section in Fig. 3): below, the earthquakes propagate roughly toward the summit, almost radially to it (from the northwest towards the southeast), while above D2 they rather propagate tangentially along an axis oriented 30° from north. These observations suggest the existence of an important geological discontinuity (D2) at that depth along the main path of migration and below Tcr.

Above discontinuity D2, we observe a region of very high seismicity where most of the seismic energy was released during the crisis and where most of the events with a magnitude larger than 1.5 occurred (histograms in Fig. 3). The vertical migration continued through this zone at a slightly lower mean velocity of 1.25 ± 0.09 m min^{-1} (0.075 km hr^{-1}) until 10:00, 1 hr before the beginning of lava outflow. A striking feature revealed by the lateral distribution of hypocentres in this zone is the elongation of the seismicity in the azimuth 30° from north which is the same orientation as the alignment connecting craters Hudson, Kapor and Krafft, and also as the orientation of the eruptive fissures which appeared above crater Kapor at the beginning of the eruption. The region of high seismicity becomes active during the first peak observed in the number of events (Fig. 6) at about 00:00 on March 9. The detailed spatiotemporal evolution of the hypocentres between 00:00 and 10:18 shown in Fig. 7 outlines that the activity is first focused in the southern part of the future cluster of events. Then during the second peak of activity starting at about 03:00 the activity shifts back to the central part of the cluster and propagates northeastwards towards sea level. Assuming that the earthquakes reflect the migration of magma towards the surface, we may interpret the above observation as magma trying first to move to the south and next to the north. This change in the propagation is probably due to a spatially varying stress field or spatially varying fracture properties making the propagation easier to the north. The first path is oriented in the direction of the Hudson vent, where the eruption started only 3 days later, and the second to the Kapor–Krafft area. The hypothesis of the first path being towards the Hudson is also supported by the presence of earthquakes below this area during the days following the beginning of the Kapor–Krafft eruption which suggests that magma continued its propagation towards the Hudson eruption site during these days.

Fig. 8 shows the comparison of waveforms for a shallow earthquake (above sea level) and those for an earthquake whose hypocentre is below the high-seismicity zone (3.5 km bsl). The waveforms are presented with amplitudes corrected for instrument

Downloaded from https://academic.oup.com/gji/article/161/2/549/1995870 by CNRS - ISTO user on 08 March 2022

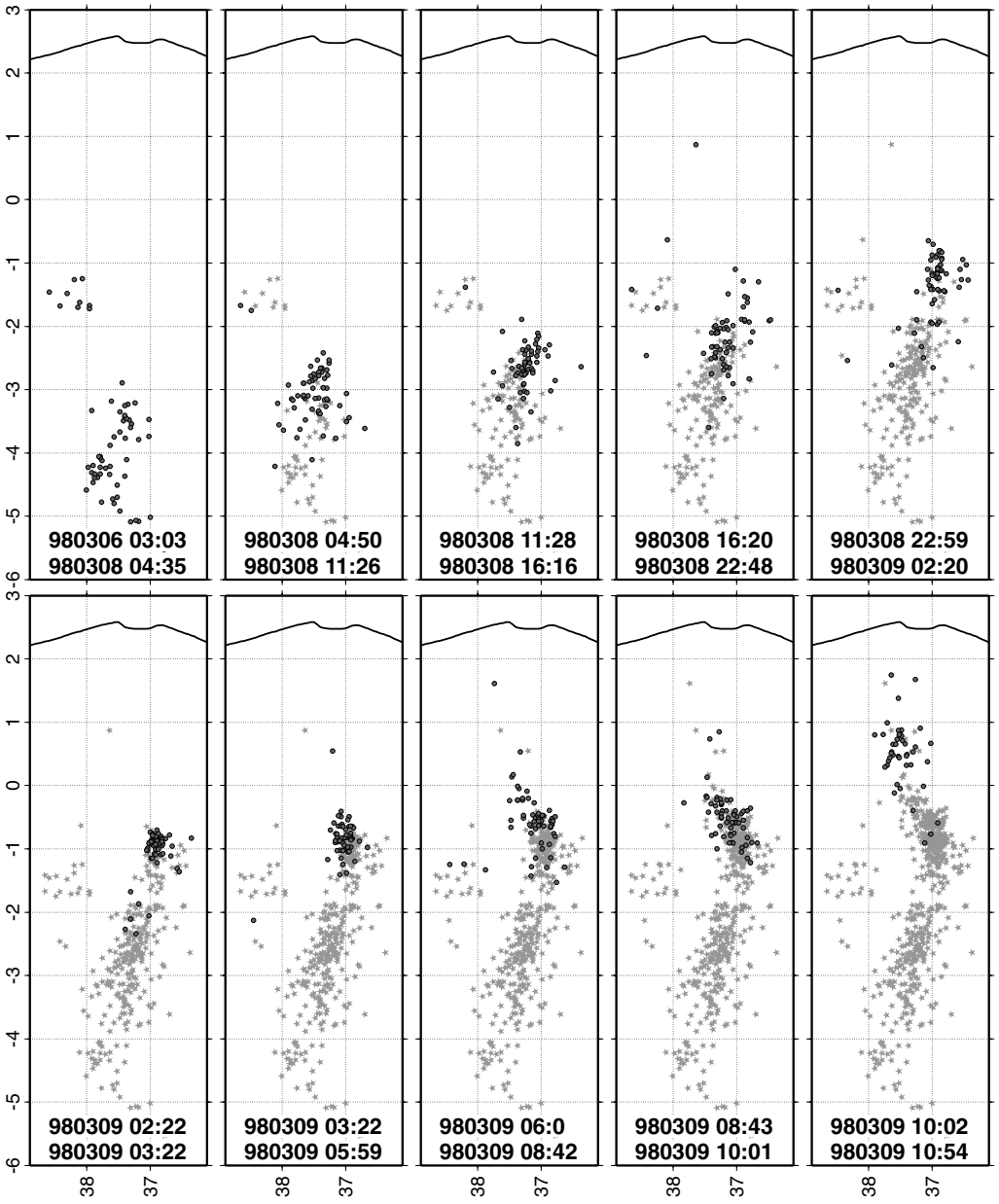

Figure 6. Spatial and temporal evolution of the located hypocentres along the north–south cross-section (part of the cross-section shown in Fig. 3). Each plot shows by black marks the events which occurred between the dates given at the bottom of the plot. In addition, the events which occurred prior to those 100 earthquakes are plotted by grey marks. The lower-right plot shows all the located events of the pre-eruption swarm.

magnification and recording site effects using coda site amplification factors calculated by Aki & Ferrazzini (2000). For the shallow event, the amplitude of the waveforms decays proportionally to the distance to the source. On the other hand, for the deeper event, amplitudes are larger at stations situated away from the summit such as PER, Pbr, Phr or Ncr while the waveforms at the summit stations Sfr, Bor and Dsr, situated closer, are attenuated. This suggests the presence of a zone of high attenuation for seismic waves below sea level. We note that, similarly, an attenuation zone has been observed below the summit of Unzen volcano (Umakoshi *et al.* 2001) and was correlating well with a low-seismicity zone. Also, Roberts *et al.* (1995) observed the presence of a high attenuation zone below Valles Caldera, New Mexico that they associated with the presence of partially fluid-saturated caldera fill material. In the present case the attenuation mostly affects earthquakes deeper than 1 km bsl, suggesting a good spatial correlation with the high-seismicity zone. Further investigation is, however, required to determine the spatial extent of this zone.

At 10:00 the activity moved clearly above sea level and we see no systematic migration of the hypocentres which are spread between sea level and the summit of the central cone (2500 m). Also, the zone of seismicity above sea level is not situated in the continuous extrapolation of the one below which is more to the west. It corresponds to the volume where most of the background seismicity is usually observed in between eruptions (Fig. 2), but also to the volume commonly activated during the short-duration pre-eruptive crises preceding the eruptions of Piton de la Fournaise. However, during the present pre-eruptive crisis, the activation of the summit

Downloaded from https://academic.oup.com/gji/article/161/2/549/1995870 by CNRS - ISTO user on 08 March 2022

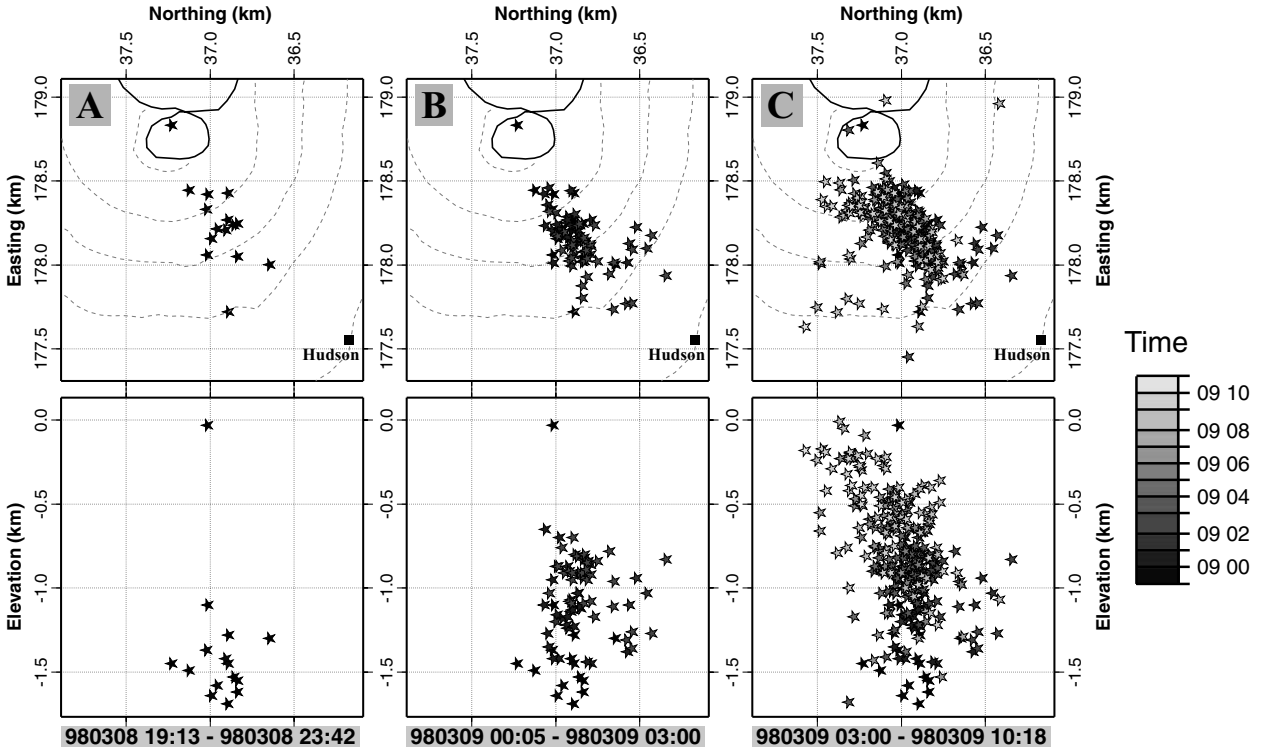

Figure 7. Spatial and temporal migration of the earthquakes in the high-seismicity zone located between 1.5 km depth and sea level. Hypocentres are shown using different shades of grey depending on their time of occurrence (time scale is given in day and hour). The three plots show: (A) initiation of the activity in the high-seismicity zone, (B) propagation toward the Hudson crater (southwest) and (C) propagation toward the site of the March 9 eruption (northeast).

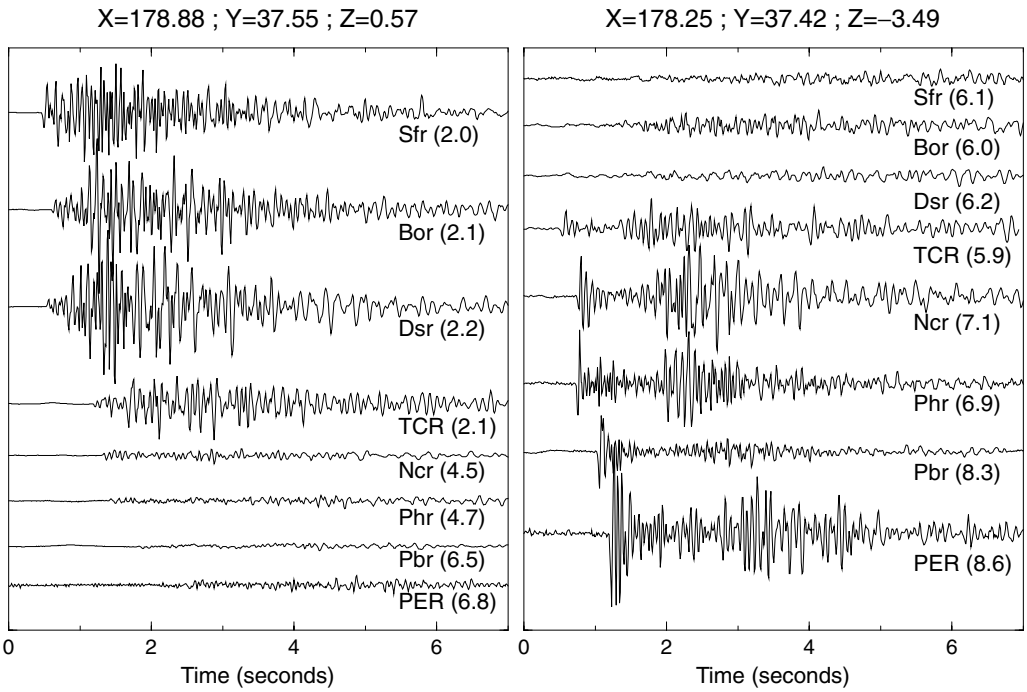

Figure 8. Comparison of waveforms recorded for an event located above sea level (left), below the summit, and those for an event recorded at 3.5 km depth (right). Waveforms are presented with a common vertical scale, after correcting for instrument magnification and recording site effects. The locations of the hypocentres are given in the upper part of each plot. The distance between the hypocentre and each station is given beside the name of the station.

structure was accompanied by the presence of a low-frequency pre-eruptive tremor, peaked around 1 Hz, which is not usually observed during pre-eruptive swarms of the Piton de la Fournaise (Battaglia 2001). Sea level appears as a major geological discontinuity (D3) which also corresponds to a low-seismicity zone. We note that, sea level corresponds more or less, in the case of the Piton de la Fournaise, to a horizon of neutral buoyancy where the magma density equals that of the surrounding medium. This horizon lies at about

Downloaded from https://academic.oup.com/gji/article/161/2/549/1995870 by CNRS - ISTO user on 08 March 2022

3 km below the surface in the case of basaltic volcanoes (Tilling & Dvorak 1993) and has been shown to match well the depth of the top of the summit reservoir at Kilauea, Mauna Loa and Krafla (Tryggvason 1984).

Except for one long-period event recorded at 06:19 on March 9, all the events detected during the pre-eruptive crisis, both above and below sea level, had high-frequency tectonic characteristics. They usually show both compressional and dilational *P*-wave arrivals suggesting that they are not caused by impulsive pressure changes directly related to the opening of the dyke but rather by shear along faults in its vicinity.

5 EARTHQUAKES AND MAGMA MIGRATION

The good match between the seismicity and the onset of the eruption suggests that it was caused by the migration of magma towards the surface. However, the notably different characteristics of the seismicity above and below sea level indicate possible different relations between the seismicity and magma transport.

Below sea level, the seismic activity outlines an almost continuous narrow vertical path which could be interpreted as a magmatic conduit linking the shallow part of the volcano to the deeper feeding system. The seismicity migrates during the swarm along that path and appears to be mostly generated at the tip of the upward-propagating conduit as activity vanishes gradually down the tip (Fig. 6). Earthquakes may be induced by stress changes related to the propagation of a batch of magma that reopens or enlarges an already existing conduit or creates a new one. It is commonly admitted that such a propagation will occur through the ascent of a dyke. We, however, note that the observed seismicity has a relatively small lateral extent with respect to its entire vertical extent, suggesting a rather narrow dyke or an almost linear or cylindrical structure, rather than a planar one. In the case of a dyke, Rubin & Gillard (1998) showed that the stress state most conducive to failure occurs near the "tip cavity", a low-pressure zone where magma cannot penetrate. This suggests that the seismicity we observe may indicate the position of the uppermost extremity of the propagating dyke. They, however, showed that the induced stress is not sufficient to cause shear failure of intact rock and that most of dyke-induced seismicity should be interpreted as resulting from slip along suitably aligned pre-existing fractures. Also, the generation of earthquakes of magnitude that can be detected requires the presence of a substantial pre-existing differential stress. Rubin & Gillard (1998) concluded that dyke-induced seismicity does not reflect the extent of the dyke, which may explain the laterally limited spatial extent of the seismicity observed in our case. Hill (1977) proposed that slip may occur along favourably oriented faults connecting *en echelon* dyke segments. In this context, the propagation of the VT activity is directly representative of the magma migration.

The mean migration velocities observed for earthquakes are about 1.2–1.6 m min^{-1} during March 8 and 9. An even slower velocity is suggested by the evolution of the few hypocentres located during the early stage of the swarm, on March 6 and 7, at about 0.4 m min^{-1}. These values are about an order of magnitude lower than velocities observed at several other volcanoes. In Hawaii, Koyanagi *et al.* (1988) deduced from the seismicity that preceded the January 1983 Kilauea eruption a downrift migration of earthquakes at a rate of 10 to 11.6 m min^{-1} (0.6 to 0.7 km hr^{-1}) during two swarms separated by a period of occasional migration. For the same pre-eruptive crisis, Okamura *et al.* (1988) deduced from tilt observations that the dyke propagated laterally at about 9.2 m min^{-1} (0.55 km hr^{-1}) and vertically at about 1.2 m min^{-1} (0.07 km hr^{-1}). For Krafla, Iceland, intrusions are accompanied by continuous tremor mixed with swarms of small earthquakes mainly occurring near the front of the migrating dyke tip. Propagation velocities of 30–72 m min^{-1} (1.8–4.3 km hr^{-1}) have been determined for those earthquakes (Brandsdóttir & Einarsson 1979; Einarsson & Brandsdóttir 1980).

The greater velocities mentioned above are, however, related to shallower areas where lithostatic pressure is lower and to rift zone areas that are highly fractured and thus may more easily allow dyke propagation. They also correspond to lateral propagations when ours is a vertical one. Magma transport may also occur through different geometries depending on the depth: a pipe-like structure at depth and crack-like for shallow areas. The crack like propagation, or dyke propagation, is a well-recognized process of transport, but is not clearly imaged by the seismicity below sea level which suggests a narrow, more cylindrical or pipe-like geometry. The pipe propagation may rather correspond to the reopening or enlargement of a pre-existing conduit, possibly partially molten, with seismicity generated in the surrounding brittle medium. The difference in stress concentration at the tip of those different geometries is a possible cause for the difference of observed propagation velocity. Higher velocities of about 12 m min^{-1} (mean velocity) and up to 120 m min^{-1} (maximum velocity) have been deduced from tilt measurements for dyke propagation in shallow areas of the Piton de la Fournaise (Toutain *et al.* 1992; Battaglia & Bachèlery 2003). Values more comparable to the velocities observed below sea level in the present case were recorded during the initial phase of the 2000 eruption of Miyakejima volcano, Japan, when earthquakes propagated away from the volcanic centre over several days at about 5 km day^{-1} (0.2 km hr^{-1} or 3.5 m min^{-1}) down to a depth of about 10–15 km (Toda *et al.* 2002).

Above sea level, the activity was of a very short duration, lasting for only an hour before the appearance of tremor originating from the eruption site. If we assume that magma travelled from sea level to the surface during that last hour we will obtain a high vertical intrusion rate of about 2.5 km hr^{-1}. An alternative explanation is that at least a part of the migration above sea level may be due to some stress transfer within magma already present below the summit. The low-frequency pre-eruptive tremor peaking at 1 Hz observed during the activation of the summit structure could be caused by fast magma transport and induced flow instabilities or alternatively by the pressurization and filling of the summit plumbing system. We note that another interpretation for the presence of this pre-eruptive tremor, uncommon at the Piton de la Fournaise, was proposed by Aki & Ferrazzini (2000) who suggested it was related to magma trying to flow into the rift zones until the eruption broke out in the summit area. The hypothesis of stress transfer into some old magma is supported by the fact that the chemical composition of the magma emitted during the first months of the eruption is the same as that of eruptions since 1977 (Bachèlery 1999), suggesting that magma was already present in the shallow plumbing system. Also, the dyke characteristics deduced from tilt data show that the dyke at the origin of the eruption propagated radially from below the summit at about 1 km above sea level and not directly from sea level (Battaglia & Bachèlery 2003). The VT seismicity in the shallow part of the volcano is scattered rather than generated in the vicinity of the propagating dyke and does not describe the propagation of the magma.

Downloaded from https://academic.oup.com/gji/article/161/2/549/1995870 by CNRS - ISTO user on 08 March 2022

6 CONCLUSIONS AND DISCUSSION

We located 583 earthquakes recorded during the seismic crisis which preceded the 1998 March 9 eruption of the Piton de la Fournaise volcano. The eruption was preceded by a seismic crisis which lasted for more than 35 hr, unusually long for this volcano, and included more than 3100 events. The locations show a monotonic upward migration of the hypocentres from about 5 km bsl to sea level with mean upward velocities of about 1.2–1.6 m min^{-1}, leading to a short-duration activity below the central cone above sea level and to the eruption 1 hr later. The shallow seismicity below the summit showed no clear migration.

The locations below sea level define an almost vertical conduit and provide unique insights into areas of the volcano where no activity has been observed since the installation of the volcano observatory and the beginning of seismic monitoring in 1980. Beside the starting depth of the crisis, 5–6 km bsl, which approximately corresponds to the depth of the interface between the island and the pre-existing oceanic crust, the VT seismicity outlines two major discontinuities at about 1.5 km bsl and at sea level. Those discontinuities appear as low-seismicity zones and are separated by a layer of high seismicity where most of the larger-magnitude events occurred. This layer also corresponds to the top of a high-attenuation zone for seismic waves. There, the activity first migrates toward the site where the Hudson eruption occurred 2.5 days later, at the end of March 11, and secondly toward the summit and the site of the March 9 eruption.

The March 9 eruption appears to have been triggered by the supply of new magma from a depth around 5–6 km bsl. However, the lavas emitted until the middle of May 1998 at this eruption site correspond to the group of the steady state basalts (Albarède *et al.* 1997) similar to those erupted since 1977. On the other hand the magma erupted at the site of the March 11 eruption was more primitive (Vlastélic *et al.* 2005) and may correspond to part of the newly supplied material. In this context, the seismicity below sea level can be interpreted as reflecting the upward propagation of new magma towards the surface, until it reaches sea level where it increases the pressure in the shallow plumbing system where some older material is already present. This process led to the eruption 1 hr later and older magma was first expelled until mid-May when newer material started appearing (Bachèlery 1999). The path leading to the March 11 Hudson eruption must have been independent of the shallow storage system. The propagation of the newer material to the Hudson eruption site must have occurred directly from the southern tip of the high-seismicity zone, triggering the earthquakes recorded between March 9 and the end of March 11.

The relatively high and slowly migrating seismicity below sea level supports the idea of difficult propagation of the magma. This is in good agreement with the fact that the eruption followed a relatively long period without eruption which could be due to the closing of the deeper feeding conduit. However, we observed a significant increase of seismicity during 1997 and also two minor seismic swarms, one in November 1996 and a second one in August 1997, which were situated above sea level, suggesting that the summit magma plumbing system was activated prior to March 1998. The possibility of an aseismic supply from depth (Hardee 1987) during the year(s) preceding the eruption is compatible with a pre-eruptive seismicity caused by the enlargement of an already existing conduit or opening of a new conduit. However, this hypothesis is not supported by the absence of long-term inflation of the summit (observatory data). An alternative explanation is that the shallow seismicity was induced by the circulation of magma at deeper levels like the starting depth of the pre-eruptive crisis. The path of magma in a volcano is usually associated with a high-velocity, high-density material such as the high-velocity plug observed by Nercessian *et al.* (1996) under Dolomieu crater. These structures may act as a stress guide and cause a stress concentration at the junction of several magma paths, as for example in the summit area. Another possibility is that the arrival of new magma at depth may also change the water circulation in the volcanic edifice and induce seismicity.

ACKNOWLEDGMENTS

We are grateful to the staff of the Observatoire Volcanologique du Piton de la Fournaise for their help in providing high-quality seismic data. Constructive reviews by two anonymous reviewers helped improve the quality of this manuscript. Thanks to Stefan Nielsen for helpful discussions.

REFERENCES

Aki, K. & Ferrazzini, V., 2000. Seismic monitoring and modeling of an active volcano for prediction, *J. geophys. Res.,* **105,** 16 617–16 640.

Albarède, F., Luais, B., Fitton, G., Semet, M., Kaminski, E., Upton, B.G.J., Bachèlery, P. & Cheminée, J.-L., 1997. The geochemical regimes of Piton de la Fournaise volcano (Réunion) during the last 530 000 years, *J. Petrol.,* **38,** 171–201.

Arciniega-Ceballos, A., Valdes-Gonzalez, C. & Dawson, P., 2000. Temporal and spectral characteristics of seismicity observed at Popocatepetl volcano, central Mexico, *J. Volc. Geotherm. Res.,* **102,** 207–216.

Aspinall, W.P., Miller, A.D., Lynch, L.L., Latchman, J.L., Stewart, R.C., White, R.A. & Power, J.A., 1998. Soufrière Hills eruption, Montserrat, 1995–1997: volcanic earthquake locations and fault plane solutions, *Geophys. Res. Lett.,* **25,** 3397–3400.

Bachèlery, P., 1999. Le fonctionnement des volcans boucliers: exemple des volcans de la Réunion et de la Grande Comore, *Habilitation à diriger des recherches,* Université de la Réunion, Ile de la Réunion.

Battaglia, J., 2001. Seismic quantification of magmatic processes on the Piton de la Fournaise between 1991 and 2000, *Thèse de doctorat,* Université de Paris 7, Paris.

Battaglia, J. & Bachèlery, P., 2003. Dynamic dyke propagation deduced from tilt variations preceding the March 9, 1998 eruption of the Piton de la Fournaise volcano, *J. Volc. Geotherm. Res.,* **120,** 289–310.

Benoit, J.P. & McNutt, S.R., 1996. Global volcanic earthquake swarm database and preliminary analysis of volcanic earthquake swarm duration, *Ann. Geofis.,* **39,** 221–229.

Brandsdóttir, B. & Einarsson, P., 1979. Seismic activity associated with the September 1977 deflation of the Krafla central volcano in NE Iceland, *J. Volc. Geotherm. Res.,* **6,** 197–212.

Chouet., B., 1996. Long-period volcano seismicity: its source and its use in eruption forecasting, *Nature,* **380,** 309–316.

Einarsson, P. & Brandsdóttir, B., 1980. Seismological evidence for a lateral magma intrusion during the July 1978 deflation of the Krafla volcano in NE Iceland, *J. Geophys.,* **47,** 160–165.

Endo, E.T., Malone, S.D., Noson, L.L. & Weaver, C.S., 1981. Locations, magnitudes, and statistics of the March 20–May 18 earthquake sequence, in *The 1980 Eruptions of Mount St. Helens, Washington,* US Geological Survey Professional Paper 1250, pp. 93–108, eds. Lipman, P.W. & Mullineaux, D.R., US Geological Survey, Washington, DC.

Gallart, A., Dryad, L., Charvis, P., Sapin, M., Hirn, A., Diaz, J., de Voogd, B. & Sachpazi, M., 1999. Perturbation to the lithosphere along the hotspot track of La Réunion from an offshore-onshore seismic transect, *J. geophys. Res.,* **104,** 2895–2908.

Downloaded from https://academic.oup.com/gji/article/161/2/549/1995870 by CNRS - ISTO user on 08 March 2022

Gardner, C.A. & White, R.A., 2002. Seismicity, gas emission and deformation histories from 18 July to September 25 1995 during the initial phreatic phase of the eruption of the Soufrière Hills Volcano, Montserrat, in *The eruption of the Soufrière Hills Volcano, Montserrat, from 1995 to 1999,* British Geological Society Memoir 21, pp. 567–581, eds Druitt, T.H. & Kokelaar, B.P., British Geological Society, London, UK.

Hardee, H.C., 1987. Heat and mass transport in the East-Rift-Zone magma conduit of Kilauea volcano, in *Volcanism in Hawaii,* US Geological Survey Professional Paper 1350, pp. 1471–1486, eds Decker, R.W., Wright, T.L. & Stauffer, P.H., US Geological Survey, Washington, DC.

Harlow, D.H., Power, J.A., Laguerta, E.P., Ambubuyong, G., White, R.A. & Hoblitt, R.P., 1996. Precursory seismicity and forecasting of the June 15, 1991, eruption of Mount Pinatubo, in *Fire and Mud, Eruptions and Lahars of Mount Pinatubo, Philippines,* pp. 285–306, eds Newhall, C.G. & Punongbayan, R.S., PHIVOLCS and University of Washington Press, Seattle, WA.

Hill, D.P., 1977. A model for earthquakes swarms, *J. geophys. Res.,* **82,** 1347–1352.

Hirn, A., Lépine, J.-C., Sapin, M. & Delorme, H., 1991. Episodes of pit-crater collapse documented by seismology at Piton de la Fournaise, *J. Volc. Geotherm. Res.,* **47,** 89–104.

Koyanagi, R.Y., Tanigawa, W.R. & Nakata, J.S., 1988. Seismicity associated with the eruption, in *The Puu Oo Eruption of Kilauea Volcano, Hawaii: Episodes 1 Through 20, January 3, 1983, Through June 8, 1984,* US Geological Survey Professional Paper 1463, pp. 183–235, ed. Wolfe, E.W., US Geological Survey, Washington, DC.

Lee, W.H.K. & Lahr, J.C., 1975. *HYPO71 (revised): a Computer Program for Determining Hypocenter, Magnitude, and First Motion Pattern of Local Earthquakes,* US Geological Survey Open File Report 75–311, US Geological Survey, Washington, DC.

Legrand, D., Calahorrano, A., Guillier, B., Rivera, L., Ruiz, M., Villagomez, D. & Yepes, H., 2002. Stress tensor analysis of the 1998–1999 tectonic swarm of northern Quito related to the volcanic swarm of Guagua Pichincha volcano, Ecuador, *Tectonophysics,* **344,** 15–36.

Lénat, J.-F. & Bachèlery, P., 1990. Structure et fonctionnement de la zone centrale du Piton de la Fournaise, in *Le Volcanisme de la Réunion,* pp. 257–296, ed. Lénat, J.-F., Centre de Recherches Volcanologiques, Clermont-Ferrand.

Lénat, J.-F., Bachèlery, P., Bonneville, A., Tarits, P., Cheminée, J.-L. & Delorme, H., 1989a. The December 4, 1983 to February 18, 1984 eruption of the Piton de la Fournaise (La Réunion, Indian Ocean): description and interpretation, *J. Volc. Geotherm. Res.,* **36,** 87–112.

Lénat, J.-F., Bachèlery, P., Bonneville, A. & Hirn, A., 1989b. The beginning of the 1985–1987 eruptive cycle at Piton de la Fournaise (La Réunion); new insights in the magmatic and volcano-tectonic systems, *J. Volc. Geotherm. Res.,* **36,** 209–232.

Nercessian, A., Hirn, A., Lépine, J.-C. & Sapin, M., 1996. Internal structure of Piton de la Fournaise volcano from seismic wave propagation and earthquake distribution, *J. Volc. Geotherm. Res.,* **70,** 123–143.

Okamura, A.J., Dvorak, J.J., Koyanagi, R.Y. & Tanigawa, W.R., 1988. Surface deformation during dyke propagation, in *The Puu Oo Eruption of Kilauea Volcano, Hawaii: Episodes 1 Through 20, January 3, 1983, Through June 8, 1984,* US Geological Survey Professional Paper 1463, pp. 165–181, ed. Wolfe, E.W., US Geological Survey, Washington, DC.

Power, J.A., Lahr, J.C., Page, R.A., Chouet, B.A., Stephens, C.D., Harlow, D.H., Murray, T.L. & Davies, J.N., 1994. Seismic evolution of the 1989–1990 eruption sequence of Redoubt Volcano, Alaska, *J. Volc. Geotherm. Res.,* **62,** 69–94.

Ratdomopurbo, A. & Poupinet, G., 2000. An overview of the seismicity of Merapi volcano (Java, Indonesia), 1983–1994, *J. Volc. Geotherm. Res.,* **100,** 193–214.

Roberts, P.M., Aki., K. & Fehler, M.C., 1995. A shallow attenuating anomaly inside the ring fracture of the Valles Caldera, New Mexico, *J. Volc. Geotherm. Res.,* **67,** 79–99.

Rubin, A.M. & Gillard, D., 1998. Dike induced seismicity: theoretical considerations, *J. geophys. Res.,* **103,** 10 017–10 030.

Rubin, A.M., Gillard, D. & Got, J.-L., 1998. A reinterpretation of seismicity associated with the January 1983 dike intrusion at Kilauea volcano, Hawaii, *J. geophys. Res.,* **103,** 10 003–10 015.

Sapin, M., Hirn, A., Lépine, J.-C. & Nercessian, A., 1996. Stress, failure and fluid flow deduced from earthquakes accompanying eruptions at Piton de la Fournaise volcano, *J. Volc. Geotherm. Res.,* **70,** 145–167.

Staudacher, T., Bachèlery, P., Semet, M.P. & Cheminée, J.-L., 1998. Piton de la Fournaise, *Bull. Global Volcanism Network, Smithsonian Institution,* **23,** 2–4.

Stieltjes, L. & Moutou, P., 1989. A statistical and probabilistic study of the historic activity of the Piton de la Fournaise, Réunion Island, Indian Ocean, *J. Volc. Geotherm. Res.,* **36,** 67–86.

Tait, S., Jaupart, C. & Vergniolle, S., 1989. Pressure, gas content and eruption periodicity of a shallow, crystallizing magma chamber, *Earth Planet. Sci. Lett.,* **92,** 107–123.

Tilling, R.I. & Dvorak, J., 1993. Anatomy of a basaltic volcano, *Nature,* **363,** 125–133.

Toda, S., Stein, R.S. & Sagiya, T., 2002. Evidence from the AD 2000 Izu islands earthquake swarm that stressing rate governs seismicity, *Nature,* **419,** 58–61.

Toutain, J.-P., Bachèlery, P., Blum, P.-A., Cheminée, J.-L., Delorme, H., Fontaine, L., Kowalski, P. & Taochy, P., 1992. Real time monitoring of vertical ground deformation during eruptions of the Piton de la Fournaise, *Geophys. Res. Lett.,* **19,** 553–556.

Tryggvason, E., 1984. Widening of the Krafla fissure swarm during the 1975–1981 volcano tectonic episode, *Bull. Volcanol.,* **47,** 47–69.

Ukawa, M. & Tsukahara, H., 1996. Earthquake swarms and dike intrusions off the east coast of Izu Peninsula, central Japan, *Tectonophysics,* **108,** 323–337.

Umakoshi, K., Shimizu, H. & Matsuwo, N., 2001. Volcano-tectonic seismicity at Unzen Volcano, Japan, 1985–1999, *J. Volc. Geotherm. Res.,* **112,** 117–131.

Vlastélic, I., Staudacher, T. & Semet, M., 2005. Rapid change of lava composition from 1998 through 2002 at Piton de la Fournaise (Réunion Island) inferred from Pb isotopes and trace elements: evidence for variable crustal contamination, *J Petrol.,* **46**(1), 79–107, doi:10.1093/petrology/egh062.

Zobin, V.M., González Amezcua, M., Reyes Dávila, G.A., Dominguez, T., Cerda Chacón, J.C. & Chávez Álvarez, J.M., 2002. Comparative characteristics of the 1997–1998 seismic swarms preceding the November 1998 eruption of Volcán de Colima, México, *J. Volc. Geotherm. Res.,* **117,** 47–60.

Downloaded from https://academic.oup.com/gji/article/161/2/549/1995870 by CNRS - ISTO user on 08 March 2022